Signatures of Nontrivial Pairing in the Quantum Walk of Two-Component Bosons

Mrinal Kanti Giri,[1] Suman Mondal,[1] B. P. Das,[2,3] and Tapan Mishra[1,2,4,*]
[1]Department of Physics, Indian Institute of Technology, Guwahati-781039, India
[2]Centre for Quantum Engineering Research and Education, TCG Centres for Research and Education in Science and Technology, Sector V, Salt Lake, Kolkata 70091, India
[3]Department of Physics, School of Science, Tokyo Institute of Technology, 2-1-2-1-H86, Ookayama, Meguro-ku, Tokyo 152-8550, Japan
[4]National Institute of Science Education and Research, HBNI, Jatni 752050, India

(Received 12 September 2021; revised 16 January 2022; accepted 8 July 2022; published 26 July 2022)

Nearest neighbor bosons possessing only on-site interactions do not form on-site bound pairs in their quantum walk due to fermionization. We obtain signatures of nontrivial on-site pairing in the quantum walk of strongly interacting two component bosons in a one dimensional lattice. By considering an initial state with particles from different components located at the nearest-neighbor sites in the central region of the lattice, we show that in the dynamical evolution of the system, competing intra- and intercomponent on-site repulsion leads to the formation of on-site intercomponent bound states. We find that when the total number of particles is three, an intercomponent pair is favored in the limit of equal intra- and intercomponent interaction strengths. However, when two bosons from each species are considered, intercomponent pairs and trimer are favored depending on the ratios of the intra- and intercomponent interactions. In both cases, we find that the quantum walks exhibit a reentrant behavior as a function of intercomponent interaction.

DOI: 10.1103/PhysRevLett.129.050601

Introduction.—The phenomenon of quantum walk (QW) has attracted much attention recently due to its importance in fundamental science as well as quantum information [1,2]. The propagation of quantum particles in different sites obeying the superposition principle of quantum mechanics makes the QW superior compared to its classical counterpart [3]. Although there are two types of QW known as discrete and continuous-time QW that have been proposed [1], the framework of continuous-time QW (CTQW) provides a versatile approach to study the dynamical properties of quantum mechanical particles in a lattice at a few particle levels. Owing to their accessibility in both theoretical and experimental approaches, the CTQW has been studied and observed in disparate systems such as ion traps, trapped neutral atoms, photonic lattices, optical waveguides, and superconducting circuits [4–15].

Recent studies on periodic lattices show that the QWs of more than one indistinguishable particle exhibits nontrivial correlations due to Hanbury Brown–Twiss (HBT) interference [13,16]. From theoretical and experimental studies, it is well established that when the walkers start from the same site, the individual particle wave packets spread ballistically and symmetrically from their initial positions. However, when the walkers are at two nearest neighbor (NN) sites, they propagate together, exhibiting the phenomenon of bosonic bunching. Further developments in studying the QWs of interacting particles have enabled us to gain insights into the combined effects of interactions, particle statistics, and strong correlations [17–21]. Interestingly, the presence of interactions between the particles leads to a completely different scenario in the QW which has recently been studied in the context of the Bose-Hubbard models in one-dimension [13,22]. It has been shown that two strongly interacting bosons on a single site exhibit QW of bound bosonic pairs, whereas two NN bosons show a transition from boson to fermion like spatial correlations and antibunching with an increase in on-site interaction [15,16]. Moreover, the QW of two NN bosons in the presence of NN interaction exhibits the signatures of a NN pair [23,24]. On the other hand, the QWs of two interacting distinguishable particles have also been explored in one dimension [25–28] exhibiting features qualitatively similar to the QW of indistinguishable particles.

An important inference that can be drawn from the existing findings is that strongly interacting NN bosons do not form local pairs in their QW. However, in this Letter, we show that in the case of the QW of two-component bosons in one dimension, nontrivial local bound pairs can be formed due to the interplay of inter- and intracomponent interactions. By considering different initial states of more than two particles, we show that the quantum correlation along with competing interactions favors the formation of on-site intercomponent bound pairs even if the two components start their QW from the NN sites. Depending on the initial conditions the formation of bound pairs are found to be more robust when suitable hopping asymmetry is introduced. Moreover, we obtain a reentrant feature in the QW as a function of the interspecies interaction.

Model.—Our analysis is based on the two-component Bose-Hubbard model which is given as

$$H = -\sum_{\langle i,j\rangle,\sigma} J_\sigma (a^\dagger_{i,\sigma} a_{j,\sigma} + \text{H.c.}) + U_{\uparrow\downarrow} \sum_i n_{i,\uparrow} n_{i,\downarrow} + \sum_{i,\sigma} \frac{U_\sigma}{2} n_{i,\sigma}(n_{i,\sigma} - 1), \quad (1)$$

where $a^\dagger_{i,\sigma}(a_{i,\sigma})$ are the creation (annihilation) operators of two different components $\sigma \in (\uparrow, \downarrow)$ that can correspond to two different atoms or two hyperfine states of a single atom. $n_{i,\sigma} = a^\dagger_{i,\sigma} a_{i,\sigma}$ is the number operator at the ith site corresponding to individual component σ. Here, J_σ and U_σ are the NN hopping matrix elements and on-site intracomponent interaction energies of the individual components σ, respectively. The intercomponent interaction is denoted by $U_{\uparrow\downarrow}$. In our studies, we assume the two components as the two hyperfine states of a single atom in a state-dependent optical lattice [29]. This assumption leads to the condition $U_\uparrow = U_\downarrow = U$ and we define $\delta = J_\downarrow / J_\uparrow$ to introduce the hopping asymmetry between the states or components. Hopping asymmetry is ensured by setting $J_\uparrow > J_\downarrow$, i.e., $\delta < 1$ and we take $J_\uparrow = 1$ as the energy scale.

We study the CTQW (hereafter referred as QW) by computing experimentally relevant quantities such as the on-site densities and the two-site correlation functions. The total on-site density is defined as $n_i(t) = \langle \sum_\sigma a^\dagger_{i,\sigma} a_{i,\sigma} \rangle$. Unlike the single particle case [13,16,18], for the two-component system we compute both the interspecies density-density and intraspecies two-particle correlation function defined as

$$\Gamma^{\downarrow\uparrow}_{ij}(t) = \langle n_{i,\downarrow} n_{j,\uparrow} \rangle \quad \text{and} \quad \Gamma^{\sigma}_{ij}(t) = \langle a^\dagger_{i,\sigma} a^\dagger_{j,\sigma} a_{j,\sigma} a_{i,\sigma} \rangle, \quad (2)$$

respectively. These quantities are calculated with a time evolved state $|\Psi(t)\rangle = e^{-iHt/\hbar}|\Psi(0)\rangle$, where $|\Psi(0)\rangle$ is some initial state. The time evolution is obtained by utilizing the time evolving block decimation (TEBD) method using the matrix product states (MPS) [30,31] with appropriate numerical control parameteres, given in [32]. The simulations are carried out using the open source MPS (OSMPS) library [33,34]. In our analysis, we consider a system size of $L = 41$ except for the case of long time evolution where we take $L = 82$.

For our studies we consider two different initial states where one or two particles from different components are located at the two NN sites at the center of the lattice. The states are (i) two $\uparrow$ particles and one $\downarrow$ particle, i.e., $|\Psi(0)\rangle_{\text{I}} = a^{\dagger 2}_{0,\uparrow} a^\dagger_{1,\downarrow} |\text{vac}\rangle$ and (ii) two $\uparrow$ and two $\downarrow$ particles, i.e., $|\Psi(0)\rangle_{\text{II}} = a^{\dagger 2}_{0,\uparrow} a^{\dagger 2}_{1,\downarrow} |\text{vac}\rangle$ as depicted in Figs. 1(a) and 1(b) respectively. In the following we discuss the QWs for both the cases in detail.

Two $\uparrow$ and one $\downarrow$ particles.—In this case we consider two $\uparrow$ particles located at the central site (i.e., $i = 0$) of the lattice and a $\downarrow$ particle at the NN site on the right (i.e., $i = 1$). The initial state corresponding to this situation is $|\Psi(0)\rangle_{\text{I}}$, which is defined earlier. This choice of the initial state ensures that $U_\downarrow$ is irrelevant in the Hamiltonian of Eq. (1). In such a scenario, the competing interactions are $U_\uparrow = U$ and $U_{\uparrow\downarrow}$. We first discuss the symmetric hopping case, i.e., $\delta = 1$. In the absence of $U_{\uparrow\downarrow}$, the two components behave independently in their QWs. For large U, the two $\uparrow$ particles form a repulsively bound pair [35] and exhibit the QW of a composite particle with reduced hopping strength [13,16,22]. This situation is similar to the case of the QWs of two particles with asymmetric hopping as discussed in Ref. [27]. It is expected that with the onset of $U_{\uparrow\downarrow}$, the individual wave packets will start reflecting from each other leading to complete reflection in the limit of large $U_{\uparrow\downarrow}$. In contrast, we show that for a moderate value of $U = 10J_\uparrow$, which is sufficient to form a bound state of $\uparrow$ particles, the QW exhibits a reentrant transition as a function of $U_{\uparrow\downarrow}$ as can be seen from Fig. 2(a)(I–IV). When $U_{\uparrow\downarrow} = 0J_\uparrow$, the QW shows a slow and fast spreading of densities indicative of that of $\uparrow\uparrow$ pair and $\downarrow$ particle, respectively, which can be seen from the finite diagonal elements of the correlation matrix $\Gamma^{\uparrow}_{ij}$ as shown in

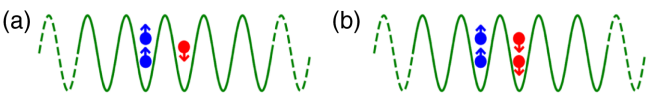

FIG. 1. The lattice diagrams (a) and (b) represent the initial state $|\Psi(0)\rangle_{\text{I}} = a^{\dagger 2}_{0,\uparrow} a^\dagger_{1,\downarrow} |\text{vac}\rangle$ and $|\Psi(0)\rangle_{\text{II}} = a^{\dagger 2}_{0,\uparrow} a^{\dagger 2}_{1,\downarrow} |\text{vac}\rangle$, respectively.

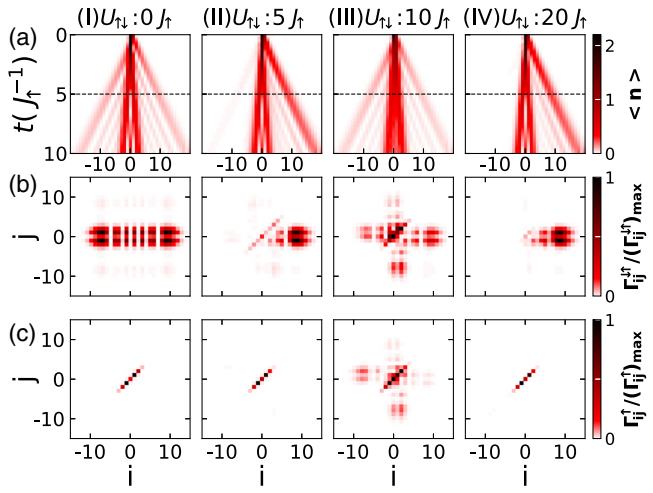

FIG. 2. Panel (a) shows the on-site density evolution with the initial state $|\Psi(0)\rangle_{\text{I}}$ for (I) $U_{\uparrow\downarrow} = 0J_\uparrow$, (II) $U_{\uparrow\downarrow} = 5J_\uparrow$, (III) $U_{\uparrow\downarrow} = 10J_\uparrow$, and (IV) $U_{\uparrow\downarrow} = 20J_\uparrow$. Panel (b) and (c) show the correlation functions $\Gamma^{\downarrow\uparrow}_{ij}$ and $\Gamma^{\uparrow}_{ij}$, respectively. Here $U = 10J_\uparrow$ and $\delta = 1$ are considered and the correlation functions are plotted at $t = 5J_\uparrow^{-1}$.

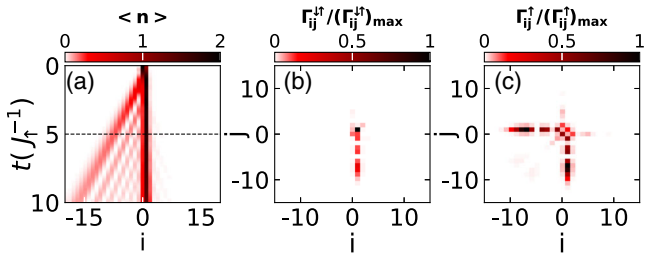

FIG. 3. Figure shows (a) $\langle n_i \rangle$, (b) $\Gamma_{ij}^{\downarrow\uparrow}$, and (c) $\Gamma_{ij}^{\uparrow}$ for the QWs with the initial state $|\Psi(0)\rangle_{\mathrm{I}}$ for $U_{\uparrow\downarrow} = 10J_{\uparrow}$, $U = 10J_{\uparrow}$, and $\delta = 0.2$. The correlation functions are plotted at $t = 5J_{\uparrow}^{-1}$.

Fig. 2(c-I). An increase in $U_{\uparrow\downarrow}$ leads to an onset of a fast spreading wave packet reflected from the slower one [Fig. 2(a-II) for $U_{\uparrow\downarrow} = 5J_{\uparrow}$], a feature which reappears when $U_{\uparrow\downarrow} > U$ [Fig. 2(a-IV) for $U_{\uparrow\downarrow} = 20J_{\uparrow}$]. This reflection of wave packet is due to the interparticle repulsion and can be understood from the vanishing of the upper triangular matrix elements of $\Gamma_{ij}^{\downarrow\uparrow}$ as shown in Fig. 2(b-II) and Fig. 2(b-IV) plotted for $U_{\uparrow\downarrow} = 5J_{\uparrow}$ and $20J_{\uparrow}$, respectively. Careful analysis of the correlation function, however, reveals that while in the limit $U_{\uparrow\downarrow} < U$ and $U_{\uparrow\downarrow} > U$, the $\uparrow\uparrow$ pair survives [see Fig. 2(c-II) and Fig. 2(c-IV)], at $U_{\uparrow\downarrow} \sim U$ it tends to break and a two-component pair (which we call a doublon, i.e., $\uparrow\downarrow$) tends to form—a scenario completely different from $U_{\uparrow\downarrow} = 0J_{\uparrow}$ limit [see Fig. 2]. This feature can be clearly seen from the gradual fading away of the diagonal elements of the intracomponent correlation matrix $\Gamma_{ij}^{\uparrow}$ [Fig. 2(c-III)] and appearance of finite diagonal elements of intercomponent density correlation matrix $\Gamma_{ij}^{\downarrow\uparrow}$ [Fig. 2(b-III)].

Interestingly, we further obtain that by reducing the hopping strength of the $\downarrow$ component compared to the $\uparrow$ component, i.e., making $\delta < 1$, breaks the $\uparrow\uparrow$ pair completely and a stable doublon is formed after a short time evolution. This doublon acts as a potential barrier that reflects the wave packet of the isolated $\uparrow$ component. These features can be seen from Fig. 3 where the density evolution and correlation functions are plotted by considering $\delta = 0.2$ while keeping $U_{\uparrow\downarrow} = U = 10J_{\uparrow}$. Note that in this case also the reentrant feature appears in the QW similar to the case of $\delta = 1$ except a noticeable change in the spreading of densities due to reflection [36].

In order to quantify the doublon formation and the dissociation of the $\uparrow\uparrow$ pair, we compute the quantities defined as

$$P_{\uparrow\downarrow} = \sum_i n_{i,\uparrow} n_{i,\downarrow}; \qquad P_{\uparrow\uparrow} = 1/2 \sum_i (n_{i,\uparrow}^2 - n_{i,\uparrow}), \tag{3}$$

which count the number of $\uparrow\downarrow$ and $\uparrow\uparrow$ pairs in the system and can be computed from the correlation matrix.

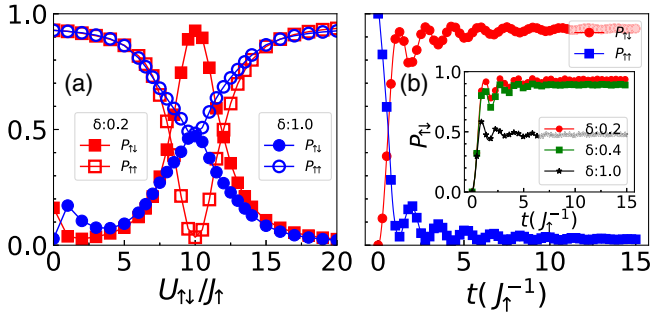

FIG. 4. (a) $P_{\uparrow\downarrow}$ (filled symbols) and $P_{\uparrow\uparrow}$ (open symbols) are plotted against $U_{\uparrow\downarrow}/J_{\uparrow}$ for $\delta = 0.2$ (red squares) and $\delta = 1.0$ (blue circles) at $t = 10J_{\uparrow}^{-1}$. (b) Shows the time evolution of $P_{\uparrow\downarrow}$ (red circles) and $P_{\uparrow\uparrow}$ (blue squares) for $\delta = 0.2$ and $U_{\uparrow\downarrow} = 10J_{\uparrow}$ indicating complete intercomponent pair formation and breaking up of $\uparrow\uparrow$ pair. (Inset) The time evolution of $P_{\uparrow\downarrow}$ for different δ such as $\delta = 0.2$ (red circles), $\delta = 0.4$ (green squares), and $\delta = 1$ (black stars).

In Fig. 4(a), we plot both $P_{\uparrow\downarrow}$ (filled symbols) and $P_{\uparrow\uparrow}$ (open symbols) as a function of $U_{\uparrow\downarrow}$ for both $\delta = 0.2$ (red squares) and $\delta = 1.0$ (blue circles) while keeping $U = 10J_{\uparrow}$, after a time evolution to $t = 10J_{\uparrow}^{-1}$. Clearly, the doublon formation is indicated by a dominant value of $P_{\uparrow\downarrow}$ at $U_{\uparrow\downarrow} = U = 10J_{\uparrow}$ for $\delta = 0.2$. Note that for $\delta = 1$, both $P_{\uparrow\downarrow}$ and $P_{\uparrow\uparrow}$ are of the same order due to the equal probabilities of formation of both the types of bound pairs. We also plot the time evolution of $P_{\uparrow\downarrow}$ and $P_{\uparrow\uparrow}$ at the critical value $U_{\uparrow\downarrow} = U = 10J_{\uparrow}$ in Fig. 4(b). The finite (zero) value of $P_{\uparrow\downarrow}$ ($P_{\uparrow\uparrow}$) after $t > 1J_{\uparrow}^{-1}$ indicates the formation (dissociation) of $\uparrow\downarrow$ ($\uparrow\uparrow$) pair. In the inset of Fig. 4(b), the variation of $P_{\uparrow\downarrow}$ for different values of δ confirms that the doublon formation is robust for smaller δ.

Summarizing up to this point, we have obtained that when $U_{\uparrow\downarrow}$ is of the order of U, the $\uparrow\uparrow$ pair tends to break, and a $\uparrow\downarrow$ pair tends to form. An introduction of hopping imbalance results in a complete dissociation of a $\uparrow\uparrow$ pair, and a doublon is formed.

The reason behind this can be explained as follows. In the limit of equal inter- and intraspecies interaction and equal hopping strengths of both the components, the binding energy of the $\uparrow\uparrow$ pair and $\uparrow\downarrow$ pair are equal. Hence the states $|(\uparrow\uparrow)_0, (\downarrow)_1\rangle$ and $|(\uparrow)_0, (\uparrow\downarrow)_1\rangle$ are degenerate. Therefore, during the QWs, when the wave packet of the $\uparrow\uparrow$ pair overlaps with that of the $\downarrow$ component there is equal probability of forming either of the bound states. Hence, we see the signature of both the $\uparrow\uparrow$ pair and $\uparrow\downarrow$ pair in the QWs. However, by making the $J_{\downarrow}$ smaller and comparable to the effective hopping strength of $\uparrow\uparrow$ pair, the doublon formation becomes energetically more favorable. This is because the doublon formation increases the overall energy of the system, and the particles avoid each other due to repulsion. Note that this phenomenon is

due to the interplay of both intra- and interspecies interactions and hence forbidden in the case of indistinguishable bosons [22] and two-component mixture with one particle from each species as considered in Ref. [27].

Two ↑ and two ↓ particles.—In this part we consider two particles from each component and study their QWs. The initial state considered for this case is given by $|\Psi(0)\rangle_{\mathrm{II}} = a^{\dagger 2}_{0,\uparrow} a^{\dagger 2}_{1,\downarrow} |\mathrm{vac}\rangle$. Note that for this initial state the $U_{\downarrow}$ term in the Hamiltonian of Eq. (1) is relevant, which was ignored previously. Now, the physics of the system will be governed by all three interactions, namely, $U_{\uparrow}$, $U_{\downarrow}$, and $U_{\uparrow\downarrow}$. Similar to the previous cases, here we assume $U_{\uparrow} = U_{\downarrow} = U = 10J_{\uparrow}$ and vary $U_{\uparrow\downarrow}$ for our investigation. We begin the discussion with asymmetric hopping and come back to the symmetric case later. In the limit of $U = 10J_{\uparrow}$, both ↑ and ↓ particles form repulsively bound pairs at the beginning when $U_{\uparrow\downarrow} = 0J_{\uparrow}$ [13,16,18,22,35]. Upon increasing the value of $U_{\uparrow\downarrow}$ with $\delta = 0.2$, we see simultaneous signatures of a three-particle and a single particle QW in the density evolution at $U_{\uparrow\downarrow} = 5J_{\uparrow}$ as shown in Fig. 5(a). The figure indicates that a ↑ particle forms a pair with an already formed ↓↓ pair leaving behind an isolated ↑ particle indicated by the central bright patch. These features can be seen in the correlation data shown in Figs. 5(b) and 5(c), where $\Gamma^{\downarrow\uparrow}_{ij}$ and $\Gamma^{\downarrow}_{ij}$ are plotted, respectively. The bright spots at (1,1) position in Figs. 5(b) and 5(c) indicate the three-particle bound state. To further quantify this we compare the behavior of $P_{\downarrow\downarrow} = 1/2 \sum_i (n^2_{i,\downarrow} - n_{i,\downarrow})$ along with $P_{\uparrow\uparrow}$ and $P_{\uparrow\downarrow}$ as a function of $U_{\uparrow\downarrow}$ in Fig. 5(g). The values of $P_{\uparrow\uparrow} \sim 0$ (blue square), $P_{\downarrow\downarrow} \sim 1$ (black diamond), and $P_{\uparrow\downarrow} \sim 2$ (red circle) for $U_{\uparrow\downarrow} = 5J_{\uparrow}$ after the time evolution to $t = 10J^{-1}_{\uparrow}$ confirm the formation of the ↑↓↓ bound state, which we call a triplon. The triplon formation can also be confirmed from the time evolved values of P's that saturate to $P_{\uparrow\downarrow} \sim 2$, $P_{\downarrow\downarrow} \sim 1$, and $P_{\uparrow\uparrow} \sim 0$ as shown in Fig. 5(h). On the other hand, the isolated ↑ particle cannot penetrate the potential barrier created by the triplon and performs a unidirectional QW on the left part of the lattice as can be seen from Fig. 5(a).

Further increase in $U_{\uparrow\downarrow}$ tends to favor the formation of all possible pairs such as the doublon (↑↓) and two intracomponent pairs (↑↑ and ↓↓) at $U_{\uparrow\downarrow} = U = 10J_{\uparrow}$. The signatures of which can be seen as the finite diagonal elements of the correlation matrices [Figs. 5(d)–5(f)] and the behavior of the values of P's [Figs. 5(g) and 5(i)]. It is to be noted that the P's exhibit finite oscillation in their time evolution for $\delta = 0.2$, which saturate fast when δ is increased [36]. The slow evolution for $\delta = 0.2$ is due to the weak effective hopping. Interestingly, we also see the signature of a nearest-neighbor ↑↓ pair in the density-density correlation matrix in Fig. 5(f). This unusual pairing

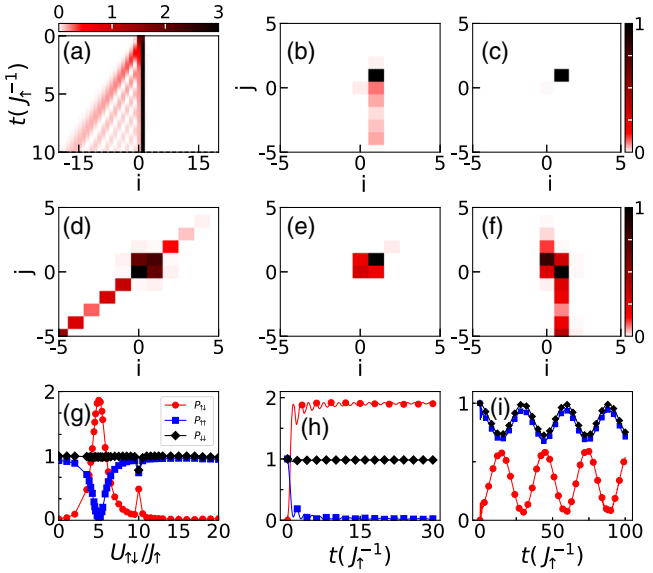

FIG. 5. Figure shows (a)$\langle n_i \rangle$, (b) $\Gamma^{\downarrow\uparrow}_{ij}$, and (c) $\Gamma^{\downarrow}_{ij}$ for the QWs with the initial state $|\Psi(0)\rangle_{\mathrm{II}}$ for $U_{\uparrow\downarrow} = 5J_{\uparrow}$, $U = 10J_{\uparrow}$, and $\delta = 0.2$ at $t = 10J^{-1}_{\uparrow}$. (d)–(f) Show the values of $\Gamma^{\uparrow}_{ij}$, $\Gamma^{\downarrow}_{ij}$, and $\Gamma^{\downarrow\uparrow}_{ij}$, respectively, for $U_{\uparrow\downarrow} = 10J_{\uparrow}$ at $t = 17J^{-1}_{\uparrow}$. (g) Shows the behavior of $P_{\uparrow\downarrow}$ (red circles), $P_{\uparrow\uparrow}$ (blue squares), and $P_{\downarrow\downarrow}$ (black diamond) as a function of $U_{\uparrow\downarrow}$ at $t = 10J^{-1}_{\uparrow}$. The time evolution of P's are plotted in (h) and (i) for $U_{\uparrow\downarrow} = 5J_{\uparrow}$ and $10J_{\uparrow}$, respectively, with $L = 82$ sites.

is inevitable due to the simultaneous formation of on-site pairs and doublons.

The triplon formation at $U_{\uparrow\downarrow} = U/2 = 5J_{\uparrow}$ can also be attributed to the condition of minimum effective interaction which can be understood as follows. In the atomic limit, the states $|(\uparrow\uparrow)_0(\downarrow\downarrow)_1\rangle$, $|(\uparrow)_0(\uparrow\downarrow\downarrow)_1\rangle$, and $|(\uparrow\uparrow\downarrow)_0(\downarrow)_1\rangle$ are degenerate. With $\delta = 0.2$, the ↑↑ pair is weakly bound compared to the ↓↓ pair because $U/J_{\uparrow} < U/J_{\downarrow}$. This ensures faster spreading of the former compared to the latter. Hence, during the time evolution, when the wave packet of the ↑↑ pair overlaps with that of the ↓↓ pair and due to degeneracy, a stable triplon is formed. Once again, at $U_{\uparrow\downarrow} = U = 10J_{\uparrow}$, the system exhibits another condition of degenerate states where the particles prefer to be in states such as $|(\uparrow\downarrow)_0(\uparrow\downarrow)_1\rangle$, $|(\uparrow\uparrow)_0(\downarrow\downarrow)_1\rangle$. In the regime when $U_{\uparrow\downarrow} < U = 5J_{\uparrow}$, $5J_{\uparrow} < U_{\uparrow\downarrow} < 10J_{\uparrow}$, and $U_{\uparrow\downarrow} > 10J_{\uparrow}$ the bosons favors to stay in the original configuration of $|(\uparrow\uparrow)_0(\downarrow\downarrow)_1\rangle$ without forming an intercomponent bound state. This is because in the limit $U_{\uparrow\downarrow} \gtrless U$ the breaking of the intracomponent pair is energetically not favorable. Note that the reentrant feature with respect to $U_{\uparrow\downarrow}$ is also present in the four particle QW [36].

On the other hand, for $\delta = 1$, the situation is completely different. Because of symmetric hopping strengths, the ↑↑ and ↓↓ pairs tend to break simultaneously and a doublon tends to form at a critical $U_{\uparrow\downarrow} = 5J_{\uparrow}$ [36]. Note that similar

to the QW with the initial state $|\Psi(0)\rangle_I$, the signature of doublon formation is weak in the four particle case with symmetric hopping strengths.

Conclusions.—In summary, our findings suggest a route to achieving local bound states in the QWs of initially nonlocal bosons with only local interactions in the context of the two-component Bose-Hubbard model. We have shown that the nontrivial intercomponent bound states can be formed at certain critical ratios of inter- and intracomponent interaction strengths. By considering three particles in total, an intercomponent bound pair is formed when both intra- and intercomponent interactions are of equal strength. However, when two particles from each component are considered, a stable triplon is formed when the interspecies interaction is half of the intraspecies ones. Moreover, we have obtained that a finite hopping asymmetry between the components plays an important role in favoring a more stable intercomponent bound pair. We have also shown that the QWs exhibit a reentrant phenomenon as a function of the intercomponent interaction.

The many-body physics of two different types of particles or two-component systems has been a topic of great interest in its own right [39] in condensed matter physics. Compared to the system with identical particles, the two-component systems are a much richer platform enabling access to a larger parameter space due to the presence of both intra- and intercomponent interactions. The present analysis opens up possibilities for further exploration in the context of the quantum walk of two component bosons such as the effects of NN interactions and disorder. Because of the rapid progress in the manipulation of ultracold binary atomic mixture in optical lattices [40–46], many physical phenomena involving two-component bosons, fermions, and Bose-Fermi mixtures have been predicted [29,47–57] and observed [8,58,59] in the framework of the Hubbard and the two-component Bose-Hubbard models. Therefore, our findings can, in principle, be simulated in a system of two-component Bose mixture in optical lattices by controlling the inter- and intracomponent interactions by the Feshbach resonance and the individual hopping strengths by the state-dependent optical lattice [29,60–63].

*mishratapan@gmail.com

[1] J. Kempe, Contemp. Phys. **44**, 307 (2003).
[2] A. M. Childs, D. Gosset, and Z. Webb, Science **339**, 791 (2013).
[3] Y. Aharonov, L. Davidovich, and N. Zagury, Phys. Rev. A **48**, 1687 (1993).
[4] H. Schmitz, R. Matjeschk, C. Schneider, J. Glueckert, M. Enderlein, T. Huber, and T. Schaetz, Phys. Rev. Lett. **103**, 090504 (2009).
[5] F. Zähringer, G. Kirchmair, R. Gerritsma, E. Solano, R. Blatt, and C. F. Roos, Phys. Rev. Lett. **104**, 100503 (2010).
[6] M. Karski, L. Förster, J.-M. Choi, A. Steffen, W. Alt, D. Meschede, and A. Widera, Science **325**, 174 (2009).
[7] C. Weitenberg, M. Endres, J. F. Sherson, M. Cheneau, P. Schauß, T. Fukuhara, I. Bloch, and S. Kuhr, Nature (London) **471**, 319 (2011).
[8] T. Fukuhara, P. Schauß, M. Endres, S. Hild, M. Cheneau, I. Bloch, and C. Gross, Nature (London) **502**, 76 (2013).
[9] K. Manouchehri and J. Wang, *Physical Implementation of Quantum Walks* (Springer, New York, 2014), 10.1007/978-3-642-36014-5.
[10] S. Hoyer, M. Sarovar, and K. B. Whaley, New J. Phys. **12**, 065041 (2010).
[11] M. Mohseni, P. Rebentrost, S. Lloyd, and A. Aspuru-Guzik, J. Chem. Phys. **129**, 174106 (2008).
[12] A. Peruzzo, M. Lobino, J. C. F. Matthews, N. Matsuda, A. Politi, K. Poulios, X.-Q. Zhou, Y. Lahini, N. Ismail, K. Wörhoff, Y. Bromberg, Y. Silberberg, M. G. Thompson, and J. L. OBrien, Science **329**, 1500 (2010).
[13] Y. Lahini, M. Verbin, S. D. Huber, Y. Bromberg, R. Pugatch, and Y. Silberberg, Phys. Rev. A **86**, 011603(R) (2012).
[14] K. Poulios, R. Keil, D. Fry, J. D. A. Meinecke, J. C. F. Matthews, A. Politi, M. Lobino, M. Gräfe, M. Heinrich, S. Nolte, A. Szameit, and J. L. O'Brien, Phys. Rev. Lett. **112**, 143604 (2014).
[15] Z. Yan, Y.-R. Zhang, M. Gong, Y. Wu, Y. Zheng, S. Li, C. Wang, F. Liang, J. Lin, Y. Xu, C. Guo, L. Sun, C.-Z. Peng, K. Xia, H. Deng, H. Rong, J. Q. You, F. Nori, H. Fan, X. Zhu, and J.-W. Pan, Science **364**, 753 (2019).
[16] P. M. Preiss, R. Ma, M. E. Tai, A. Lukin, M. Rispoli, P. Zupancic, Y. Lahini, R. Islam, and M. Greiner, Science **347**, 1229 (2015).
[17] W. S. Bakr, A. Peng, M. E. Tai, R. Ma, J. Simon, J. I. Gillen, S. Foelling, L. Pollet, and M. Greiner, Science **329**, 547 (2010).
[18] S. Mondal and T. Mishra, Phys. Rev. A **101**, 052341 (2020).
[19] P. Wrzosek, K. Wohlfeld, D. Hofmann, T. Sowiński, and M. A. Sentef, Phys. Rev. B **102**, 024440 (2020).
[20] H. Cayla, S. Butera, C. Carcy, A. Tenart, G. Hercé, M. Mancini, A. Aspect, I. Carusotto, and D. Clément, Phys. Rev. Lett. **125**, 165301 (2020).
[21] C. F. Roos, A. Alberti, D. Meschede, P. Hauke, and H. Häffner, Phys. Rev. Lett. **119**, 160401 (2017).
[22] D. Wiater, T. Sowiński, and J. Zakrzewski, Phys. Rev. A **96**, 043629 (2017).
[23] X. Qin, Y. Ke, X. Guan, Z. Li, N. Andrei, and C. Lee, Phys. Rev. A **90**, 062301 (2014).
[24] W. Li, A. Dhar, X. Deng, K. Kasamatsu, L. Barbiero, and L. Santos, Phys. Rev. Lett. **124**, 010404 (2020).
[25] W. S. Dias, E. M. Nascimento, M. L. Lyra, and F. A. B. F. de Moura, Phys. Rev. B **76**, 155124 (2007).
[26] S. Sarkar and T. Sowiński, Phys. Rev. A **102**, 043326 (2020).
[27] M. K. Giri, S. Mondal, B. P. Das, and T. Mishra, Sci. Rep. **11**, 22056 (2021).
[28] A. Peixoto and W. Dias, Solid State Commun. **242**, 68 (2016).
[29] E. Altman, W. Hofstetter, E. Demler, and M. D. Lukin, New J. Phys. **5**, 113 (2003).
[30] G. Vidal, Phys. Rev. Lett. **91**, 147902 (2003).
[31] G. Vidal, Phys. Rev. Lett. **93**, 040502 (2004).

[32] In this work, we use the TEBD method, which is a very efficient method for time evolving an initial state where the Hamiltonian consists of local and short-range terms. The fourth-order Trotterized two site gates are employed to evolve the initial states with the time step 0.01. In all the cases, we consider the maximum bond dimension of 500 and tolerance is of the order of 10^{-10}. In our simulation, we utilize the conservation of the total number of particles.
[33] M. L. Wall and L. D. Carr, New J. Phys. **14**, 125015 (2012).
[34] D. Jaschke, M. L. Wall, and L. D. Carr, Comput. Phys. Commun. **225**, 59 (2018).
[35] K. Winkler, G. Thalhammer, F. Lang, R. Grimm, J. Hecker Denschlag, A. J. Daley, A. Kantian, H. P. Büchler, and P. Zoller, Nature (London) **441**, 853 (2006).
[36] See Supplemental Material at http://link.aps.org/supplemental/10.1103/PhysRevLett.129.050601 for details, which includes Refs. [37,38].
[37] A. B. Kuklov and B. V. Svistunov, Phys. Rev. Lett. **90**, 100401 (2003).
[38] S. Mondal, S. Greschner, L. Santos, and T. Mishra, Phys. Rev. A **104**, 013315 (2021).
[39] F. H. L. Essler, H. Frahm, F. Göhmann, A. Klümper, and V. E. Korepin, *The One-Dimensional Hubbard Model* (Cambridge University Press, Cambridge, England, 2005).
[40] M. Taglieber, A.-C. Voigt, T. Aoki, T. W. Hänsch, and K. Dieckmann, Phys. Rev. Lett. **100**, 010401 (2008).
[41] E. Wille, F. M. Spiegelhalder, G. Kerner, D. Naik, A. Trenkwalder, G. Hendl, F. Schreck, R. Grimm, T. G. Tiecke, J. T. M. Walraven, S. J. J. M. F. Kokkelmans, E. Tiesinga, and P. S. Julienne, Phys. Rev. Lett. **100**, 053201 (2008).
[42] S. Ospelkaus, C. Ospelkaus, O. Wille, M. Succo, P. Ernst, K. Sengstock, and K. Bongs, Phys. Rev. Lett. **96**, 180403 (2006).
[43] K. Günter, T. Stöferle, H. Moritz, M. Köhl, and T. Esslinger, Phys. Rev. Lett. **96**, 180402 (2006).
[44] T. Best, S. Will, U. Schneider, L. Hackermüller, D. van Oosten, I. Bloch, and D.-S. Lühmann, Phys. Rev. Lett. **102**, 030408 (2009).
[45] J. Catani, L. De Sarlo, G. Barontini, F. Minardi, and M. Inguscio, Phys. Rev. A **77**, 011603(R) (2008).
[46] B. Gadway, D. Pertot, R. Reimann, and D. Schneble, Phys. Rev. Lett. **105**, 045303 (2010).
[47] A. Isacsson, M.-C. Cha, K. Sengupta, and S. M. Girvin, Phys. Rev. B **72**, 184507 (2005).
[48] L.-M. Duan, E. Demler, and M. D. Lukin, Phys. Rev. Lett. **91**, 090402 (2003).
[49] P. P. Orth, I. Stanic, and K. Le Hur, Phys. Rev. A **77**, 051601 (R) (2008).
[50] W. Wang, V. Penna, and B. Capogrosso-Sansone, New J. Phys. **18**, 063002 (2016).
[51] L. Mathey, Phys. Rev. B **75**, 144510 (2007).
[52] T. Mishra, R. V. Pai, and B. P. Das, Phys. Rev. A **76**, 013604 (2007).
[53] M. Singh, S. Mondal, B. K. Sahoo, and T. Mishra, Phys. Rev. A **96**, 053604 (2017).
[54] L. Barbiero, L. Santos, and N. Goldman, Phys. Rev. B **97**, 201115(R) (2018).
[55] S. Mondal, S. Greschner, L. Santos, and T. Mishra, Phys. Rev. A **104**, 013315 (2021).
[56] B.-T. Ye, L.-Z. Mu, and H. Fan, Phys. Rev. B **94**, 165167 (2016).
[57] M. Gärttner, A. Safavi-Naini, J. Schachenmayer, and A. M. Rey, Phys. Rev. A **100**, 053607 (2019).
[58] N. H. Le, A. J. Fisher, N. J. Curson, and E. Ginossar, npj Quantum Inf. **6**, 24 (2020).
[59] S. Scherg, T. Kohlert, J. Herbrych, J. Stolpp, P. Bordia, U. Schneider, F. Heidrich-Meisner, I. Bloch, and M. Aidelsburger, Phys. Rev. Lett. **121**, 130402 (2018).
[60] L.-M. Duan, E. Demler, and M. D. Lukin, Phys. Rev. Lett. **91**, 090402 (2003).
[61] O. Mandel, M. Greiner, A. Widera, T. Rom, T. W. Hänsch, and I. Bloch, Phys. Rev. Lett. **91**, 010407 (2003).
[62] P. Soltan-Panahi, J. Struck, P. Hauke, A. Bick, W. Plenkers, G. Meineke, C. Becker, P. Windpassinger, M. Lewenstein, and K. Sengstock, Nat. Phys. **7**, 434 (2011).
[63] B. Yang, H.-N. Dai, H. Sun, A. Reingruber, Z.-S. Yuan, and J.-W. Pan, Phys. Rev. A **96**, 011602(R) (2017).